PHOTONICS Research

Wide tunable laser based on electrically regulated bandwidth broadening in polymer-stabilized cholesteric liquid crystal

Hongbo Lu,[1,2,7] Cheng Wei,[1] Qiang Zhang,[1] Miao Xu,[1,2] Yunsheng Ding,[2] Guobing Zhang,[1,2] Jun Zhu,[1,2] Kang Xie,[3] Xiaojuan Zhang,[4] Zhijia Hu,[3,4,5,6] and Longzhen Qiu[1,2]

[1]Key Laboratory of Special Display Technology, National Engineering Laboratory of Special Display Technology, State Key Laboratory of Advanced Display Technology, Academy of Opto-Electronic Technology, Hefei University of Technology, Hefei 230009, China
[2]Key Laboratory of Advanced Functional Materials and Devices, Anhui Province, School of Chemistry and Chemical Engineering, Hefei University of Technology, Hefei 230009, China
[3]School of Instrument Science and Opto-Electronics Engineering, Hefei University of Technology, Hefei 230009, China
[4]Aston Institute of Photonic Technologies, Aston University, Birmingham B4 7ET, UK
[5]State Key Laboratory of Environment-Friendly Energy Materials, Southwest University of Science and Technology, Mianyang 621000, China
[6]e-mail: zhijiahu@hfut.edu.cn
[7]e-mail: bozhilu@hfut.edu.cn

Received 15 October 2018; accepted 24 November 2018; posted 30 November 2018 (Doc. ID 348249); published 10 January 2019

Electrically responsive photonic crystals represent one of the most promising intelligent material candidates for technological applications in optoelectronics. In this research, dye-doped polymer-stabilized cholesteric liquid crystals (PSCLCs) with negative dielectric anisotropy were fabricated, and mirrorless lasing with an electrically tunable wavelength was successfully achieved. Unlike conventional liquid-crystal lasers, the proposed laser aided in tuning the emission wavelength through controlling the reflection bandwidth based on gradient pitch distribution. The principal advantage of the electrically controlled dye-doped PSCLC laser is that the electric field is applied parallel to the helical axis, which changes the pitch gradient instead of rotating the helix axis, thus keeping the heliconical structure intact during lasing. The broad tuning range (~110 nm) of PSCLC lasers, coupled with their stable emission performance, continuous tunability, and easy fabrication, leads to its numerous potential applications in intelligent optoelectronic devices, such as sensing, medicine, and display.

https://doi.org/10.1364/PRJ.7.000137

1. INTRODUCTION

Liquid-crystal (LC) lasers have attracted significant attention in the scientific community in recent years. The broad wavelength tuning range, coupled with their microscopic size, narrow linewidth, large coherence area, and high optical efficiency, opens up new application avenues such as miniature medical diagnostic tools, sensing, informational displays, and lab-on-chip devices [1,2]. LC materials are a class of soft matter that combines crystalline-like ordering with fluid-like behavior. Due to the strong interactions among the molecules, LCs can self-assemble into different ordered mesophases, such as the common nematic and smectic phases, without the aid of any external stimulus. Introduction of the chiral center in the molecules and/or addition of some chiral dopants into nematic LCs leads to the twisting and self-assembling of the molecules into a periodic helical structure, forming cholesteric liquid crystal (CLC) with a pitch (p) in the submicrometer and micrometer range. The dielectric permittivity is periodic in space; therefore, CLCs can be seen as one-dimensional photonic crystals, which selectively reflect the specific band circularly polarized light with the same handedness as the helix. The reflection band edges are located at $\lambda_o = p \times n_o$ and $\lambda_e = p \times n_e$, where n_o and n_e are the ordinary and extraordinary refractive indices of the local uniaxial structure, respectively [3,4]. Once a laser dye is doped into the CLCs, provided that the fluorescence emission spectrum of the dye overlaps the edge of the photonic bandgap, mirrorless lasing is observed at the edge under certain pumping conditions, which is the so-called band-edge CLC laser [5–8].

One major attractive feature of CLC lasers is the tunability of the emission wavelength over a wide range via controlling the pitch. This can be obtained by changing the composition [9], position [10,11], temperature [12], and mechanical strain [13,14], and by using reversible photochemical reactions [15].

In general, a large tuning range and a rapid response rate are preferred for the LC lasers. A large wavelength shift of about 80 nm was achieved by biaxially stretching a CLC elastomer [16]. Zheng *et al.* reported that a CLC emulsion laser could be reversibly phototuned in a wide spectral range of 112 nm, and it simultaneously exhibited stable emission performance and quasi-continuous tunability [17]. As it is the most desirable mode, the electrical tunability of the emission intensity and wavelength has been widely studied. Switching of the lasing in polymer-stabilized CLCs (PSCLCs) by lowering the electric field (less than 10 V) has been reported [18]. However, the wavelength shifts are normally less than 50 nm for conventional CLC lasers using the electric field tuning method [19–23]. This is attributed to the fact that the electric field applied parallel to the helix axis, instead of changing the pitch while keeping the cholesteric axis intact for lasers, rotates this axis due to the dielectric anisotropy of the LC. This results in a light scattering structure called a "focal conic texture," which distorts the harmonic periodic helical structure and dramatically reduces the optical positive feedback [24–26]. Recently, Xiang *et al.* presented an electrically tunable laser with an extraordinarily broad range (>100 nm) in the visible spectrum based on an oblique heliconical CLC, in which the molecules formed an acute angle with the helicoidal axis rather than aligning perpendicular to it as in the conventional CLC [27].

In this study, we described electrically tunable lasing based on PSCLCs with negative dielectric anisotropy. The reflection band of the PSCLC could be broadened by direct current (DC) electric fields, which is ascribed to the pitch gradient caused by the motion of the polymer network. Importantly, the field-induced change in the pitch gradient did not change the orientation of the helical axis, which remained parallel to the applied field, and thus the regular heliconical structure was maintained. Herein, we demonstrate efficient electrical tuning of the lasing emission wavelength with an extraordinarily broad range (more than 110 nm) in dye-doped PSCLCs with pitch gradient distribution. To the best of our knowledge, such a wide electrically tunable CLC laser based on controlling the pitch gradient and utilizing the polymer network deformation has not been reported previously.

2. EXPERIMENT

A. Materials and Sample Preparation

The materials used in this study included a nematic mixture of HNG715500-000 (HCCH, China; $\Delta n = 0.075$, $\Delta\varepsilon = -14.2$ at 298 K), chiral dopant R6N (HCCH, China), photopolymerizable LC monomer RM257 (HCCH, China), and photoinitiator benzoin methyl ether (BME; TCI, Japan). The laser dye used in this study was pyrromethene 597 (PM597; Exciton, USA). The chemical structures of the materials are shown in Fig. 1(a); the absorption peak was at ~520 nm and the fluorescence peak was at ~582 nm for the PM597 in the LC mixture [Fig. 1(b)]. The optimized constituent fraction (in weight units) of PSCLC is HNG715500-000/R6N/RM257/BME/PM597=100/3.7/6.5/1.1/0.8. The mixtures were injected into vertical field switching cells by capillary action, where a cell gap of 36 μm was controlled via the dispersion of spacer beads. The cells were made of two glass substrates

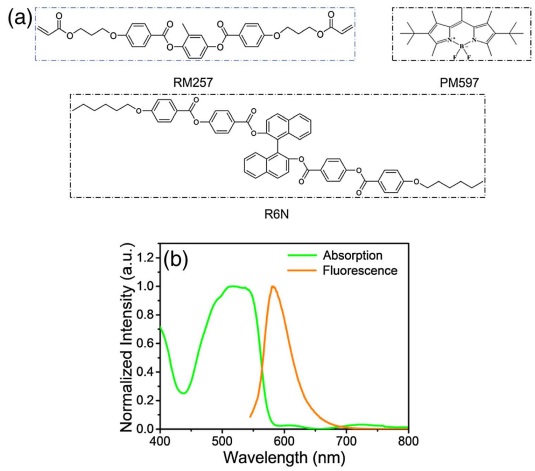

Fig. 1. Chemical structures of chiral dopant R6N, liquid-crystal monomer RM257, and laser dye pyrromethene 597 and the fluorescence spectrum and absorption spectrum of laser dye PM597 in a nematic LC mixture.

with a planar indium tin oxide (ITO) electrode. The substrates were also coated with polyimide and rubbed to generate a homogeneous alignment of the LCs. The electric fields were applied in the longitudinal direction. Before polymerization, a low-frequency alternating current (AC) electric voltage (150 V, 10 Hz) was applied on the cell for 1 min to obtain a more uniform film. Then the cells were cured by UV irradiation ($\lambda = 365$ nm, intensity 30 mW · cm^2) at 25°C for 45 min with applied high-frequency AC electric voltage (150 V, 1 kHz) to obtain a better photonic bandgap structure. The AC electric voltage was applied using a 20 MHz function/arbitrary waveform generator (Agilent 33220A, USA) with a high-speed bipolar amplifier (NF BA4825, Japan).

B. Optical Path Construction and Characterization

The transmission and reflection spectra were recorded using a UV–visible spectrophotometer (Shimadzu-UV2550, Japan). The laser spectra were analyzed using a spectrometer (QE65 Pro, Ocean Optics, USA; resolution ~0.4 nm, integration time ~100 ms). The colors of the PSCLC sample were captured using a polarized optical microscope (Leica DM2500 M, Germany). The fluorescence spectra were recorded using a spectrofluorometer (HORIBA FluoroMax-4, Japan). The optical path structure is shown in Fig. 2.

To obtain electrically tunable lasing emission, the cells were optically pumped using a pulsed frequency-doubled Nd:YAG laser with a wavelength of 532 nm. The pulse width and the

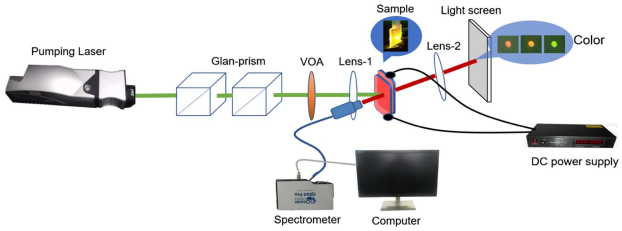

Fig. 2. Optical path structure.

repetition rate of a pump beam were 10 ns and 10 Hz, respectively. The pump beam was focused on the cell using a lens. The output lasing emission along the normal backward direction of the cell was collected into an optical fiber and analyzed using a spectrometer, and the emission beam in the forward direction was focused on the light screen. The pump pulse energy and polarization incident on the sample were controlled by a Glan prism group and an variable optical attenuator (VOA). Moreover, the DC electric field was controlled using a Keithley 2400 source (Tektronix, USA).

3. RESULTS AND DISCUSSION

In this work, the PM597-doped CLC mixtures were inserted by capillary action into 36 μm gap cells with ITO electrodes and anti-parallel-rubbed polyimide alignment layers. The filled cell displayed a planar structure in which the helical axis was aligned perpendicular to the substrate [Fig. 3(a)]. The transmission spectral measurement revealed a selective reflection band between 685 and 725 nm, which covered the edge of the fluorescence emission spectrum of PM597. When the sample was pumped using an Nd:YAG laser with a wavelength of 532 nm (pulse width and repetition rate of 10 ns and 10 Hz, respectively), a red laser located at 686 nm with a threshold of 2.76 μJ was observed in the direction of the helical axis [Figs. 3(b) and 3(c)].

Then, the cell was irradiated under UV light to form the PSCLC. During the polymerization, a high AC electric field was applied on the cell to maintain the regular helical structure. The as-formed polymer network was highly cross linked, and it was also anisotropic due to the aligning effect on the monomer exerted by the host LC and the anisotropic diffusional property of the monomer in the LC [28–30]. After the polymerization, the PSCLC was also in the planar state, and the reflection band blueshifted by about 13 nm. Correspondingly, blueshifting of the lasing wavelength to 673 nm was also observed. Moreover, the lasing threshold for the dye-doped PSCLC was 1.31 μJ, which was significantly lower than that of dye-doped CLC, 2.76 μJ [Fig. 3(c)]. This was attributed to the fact that the reflection band of the dye-doped PSCLC was closer to the peak fluorescence emission of PM597, and the polymer network reduced the vibration of the LC molecules and the energy loss.

Figure 4 illustrates the electric-field-dependent broadening of the selective reflection band of the PSCLC together with the electrical tunability of the emission wavelength of the laser. When the voltage was applied across the cell, the LC was supposed to remain in the planar state because of the negative dielectric anisotropy. When AC voltages were applied, the reflection spectrum remained unchanged and no obvious change was observed for the lasing wavelength under optical pumping. However, when DC voltages were applied, the reflection band surprisingly became wider and the laser emission wavelength blueshifted gradually [Fig. 4(b)]. The original reflection bandwidth was about 40 nm in the transmission spectrum, which is in good agreement with the theoretical prediction using the formula $\Delta\lambda = \Delta n \times p = 0.075 \times 460 = \sim 35$ nm, and the lasing was located at the short-wavelength edge of the reflection band. With the increase in voltage, the bandwidth of the selective reflection band also increased and the reflective color

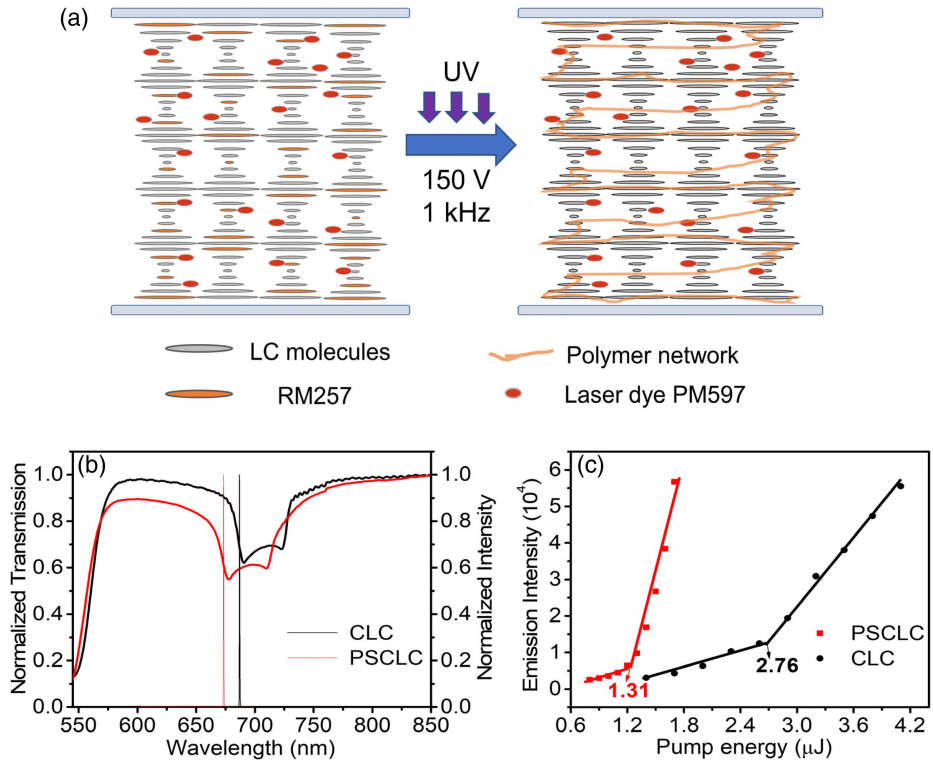

Fig. 3. Emission characteristics of lasers in the CLC and PSCLC. (a) Formation of the PSCLC, (b) the transmission and corresponding laser emission spectra of the dye-doped CLC and dye-doped PSCLC samples, and (c) the emission intensity of the lasers as a function of the pump energy.

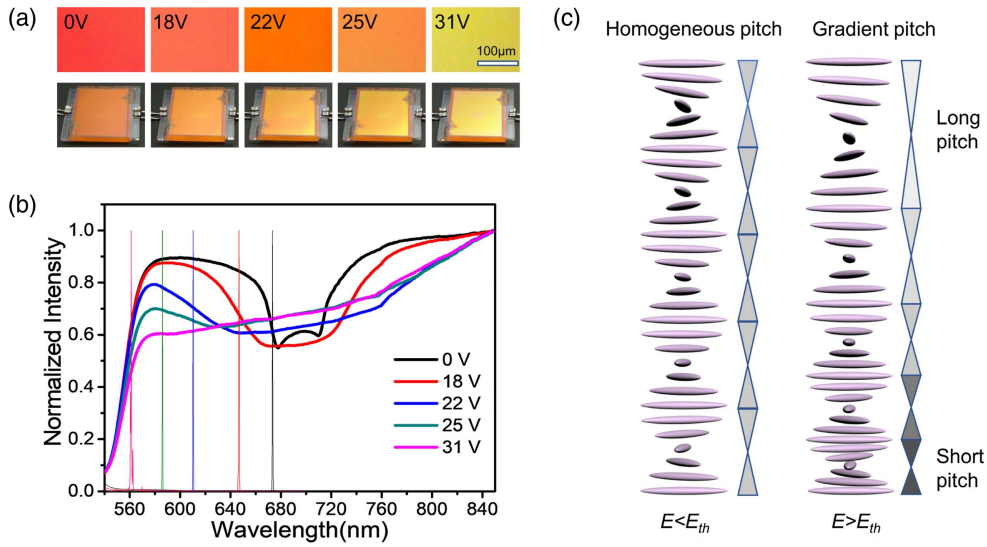

Fig. 4. Electric-field-dependent broadening of the selective reflection band together with the electrical tunability of the emission wavelength of the laser. (a) The microphotographs observed under a polarized optical microscope and photographs of the dye-doped PSCLC under various voltages, (b) the transmission and corresponding laser emission spectra of the dye-doped PSCLC under various voltages with an excited pump energy of ~1.4 μJ, and (c) the schematic illustration of the pitch distribution under different electric fields.

was tuned from deep red to light yellow, as shown in Fig. 4(a). When the voltage was increased to 31 V, the bandwidth exhibited a fivefold increase to about 210 nm, which almost covered the entire fluorescence band. Correspondingly, the lasing emission wavelength moved gradually, passing through 646 nm for 18 V, 610 nm for 22 V, and 585 nm for 25 V, until it reached 560 nm for 31 V, which was very close to the edge of the fluorescence band. Using the optical pump, the lasing emission had a typical full width at half-maximum (FWHM) in the range 0.35–0.64 nm (exact value can be seen in Table 1) and always occurred at the short-wavelength edge of the different reflection bandwidth.

The use of a DC electric field to broaden the reflection band in the PSCLC, while preserving the regular heliconical structure, provides an efficient mechanistic approach for tuning the lasing wavelength as long as the reflection band overlaps the fluorescence spectra of the laser dye. In the PSCLC, the polymer network trapped the positive ions by electrostatic force due to the polar groups [31–36]. In the absence of the applied electric field, the pitch of the CLC was uniform across the cell, which enabled a narrow band reflection. When a DC electric field was applied, the dispersed polymer network moved translationally due to an electromechanical force exerted by the electric field. The motion of the polymer network resulted in a gradient pitch distribution by stretching the pitch near the anode side and compressing it near the cathode side. Furthermore, the LC remained in the planar state because of the aligning effect of the polymer network and the negative dielectric anisotropy [Fig. 4(c)]. As a consequence, the reflection band was broadened. The laser emission wavelength followed the short-wavelength edge of the reflection band and moved toward a shorter wavelength with the increasing applied electric field. When the electric field was removed, the elastic polymer network went back to its original state and position, which showed a reversible tunability. The tunability of the laser was extraordinarily broad, as the lasing wavelength changed in the range of 558–673 nm in the PM597-doped PSCLC. The tunable range covered a large portion of the fluorescence band for the dye. In principle, with suitable laser dyes and a pump source, there is no limitation other than dispersion to extend lasing into different regions of the spectrum.

The lasing thresholds at different voltages were investigated, as shown in Fig. 5(a). The laser emission shows a clear threshold of 1.31, 1.19, and 1.35 μJ for tunable voltages of 0, 22, and 31 V, respectively. The lowest threshold is for the case of photonic bandgap (PBG) near the fluorescence peak of the laser dye, and the higher threshold is for the one far away from the fluorescence peak. The dependence of the lasing threshold on the lasing wavelength emitted from different DC electric field controlled cases is shown in Fig. 5(b). We investigated the thresholds of eight laser peak positions at about 560, 570, 585, 600, 615, 630, 645, and 673 nm, respectively. Clearly, the low threshold values are near the fluorescence peak, but they have little difference in numerical value when the laser peak is not too far away from the fluorescence peak. However, the threshold of the laser peak at 673 nm for which the sample

Table 1. Peak Position and FWHM of the Laser Obtained by Different Drive Voltages

Voltage (V)	0	17	18	20	21	22	23.5	26	30
Wavelength (nm)	673.30	659.81	646.73	627.81	613.06	602.06	589.79	573.76	561.17
FWHM (nm)	0.36	0.50	0.39	0.38	0.64	0.36	0.35	0.54	0.35

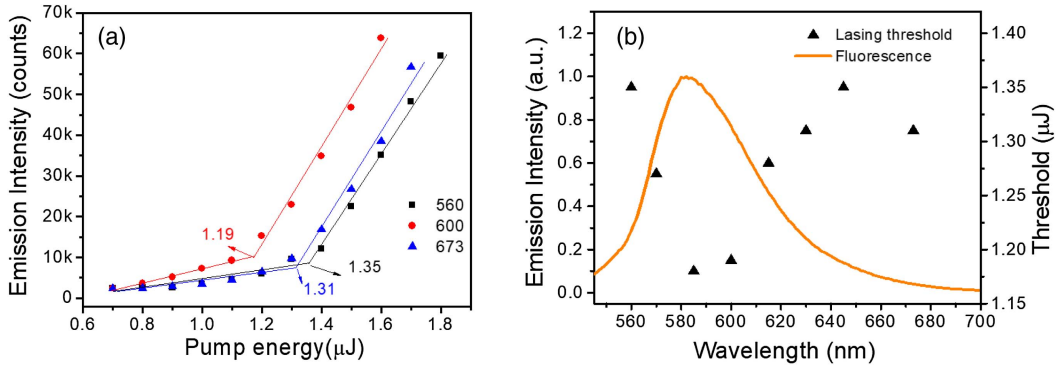

Fig. 5. (a) Lasing threshold at different wavelength positions and (b) lasing threshold distribution compared to fluorescence spectrum.

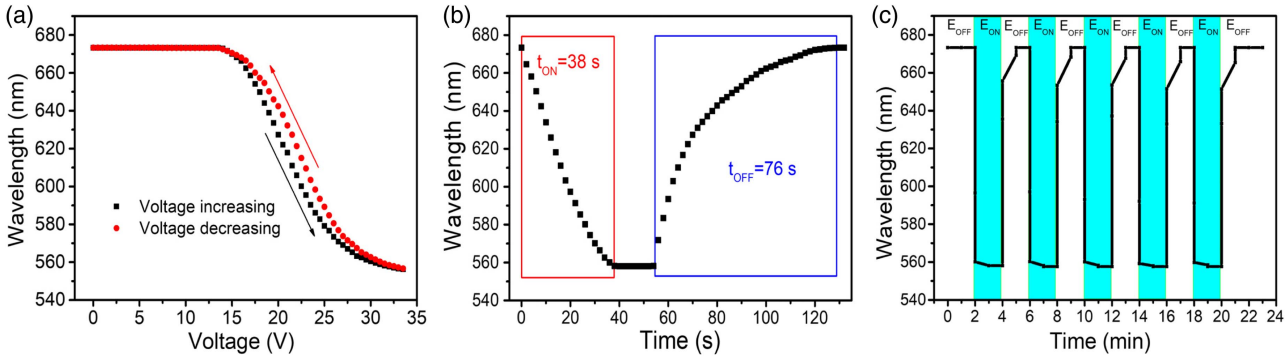

Fig. 6. Electric field response characteristics of the dye-doped PSCLC. (a) The relationship between the driving voltage and the peak wavelength of the laser, (b) the response speed of the laser, and (c) characterization of the electric field response stability when switching the electric field ON\OFF.

has not applied a DC electric field is a little higher than that for the position that is closer to the fluorescence peak. This can be attributed to its regular structure and higher number of periods.

The tunability of the laser emission from the PSCLCs depends on the motion of the polymer network, which endows some unique features such as continuous tunability. The continuous tuning of the wavelength of the laser has always been a concern for researchers, because it is difficult to achieve in conventional CLCs. This difficulty is attributed to the fact that the strong anchoring on the inner surfaces of two substrates compels the LCs near the surfaces to align in parallel, causing a discrete pitch tuning following the relationship, in which the cell gap is equal to the integer times of half of the pitch [11]. Figure 6(a) shows better continuous electrically tuned dye-doped PSCLCs. When the applied voltages exceeded the threshold of about 13 V, the electrostatic force became sufficient to drive the motion of the polymer network, and the lasing peak continuously blueshifted to 558 nm until the voltage became 33.5 V (the saturation voltage). Above the saturation voltage, the laser emission became inefficient and unstable. With a further increase in the voltage, the laser emission was completely eliminated, with the reflection band edge too far away from the fluorescence band. It can be seen that the laser peak position has a small deviation at the same voltage for the increasing and decreasing voltage processes. This hysteretic effect was attributed to the relaxation feature of the polymer network. The dynamic response characteristics of the PSCLC laser are shown in Fig. 6(b). When the electric field (33.5 V) was applied, the lasing wavelength blueshifted from ~673 nm and stabilized at ~558 nm after about 38 s. When the electric field was removed, the lasing wavelength moved back to the original position, which required about 76 s. The tunable lasing wavelength was reversible and stable in the cyclic process [Fig. 6(c)].

In order to demonstrate the characteristics of electrical tuning of the laser emission, circular polarization of the laser was investigated during the tuning process. Figure 7 presents the polarization analysis, indicating that laser radiations are all right-handed circularly polarized (RCP), which matches the right-handed helical structure of the PSCLC. Moreover, the polarization characteristics of lasers were independent of the emission wavelength. The results supported the fact that the gradient pitch distribution with a regular heliconical structure could be treated as a distributed feedback cavity and the band-edge lasing could be tailored using the photonic bandgap in the laser dye-doped PSCLCs through controlling the DC electric fields.

4. CONCLUSIONS

A wide-range electrically tunable laser based on PSCLCs with negative dielectric anisotropy was demonstrated in this study.

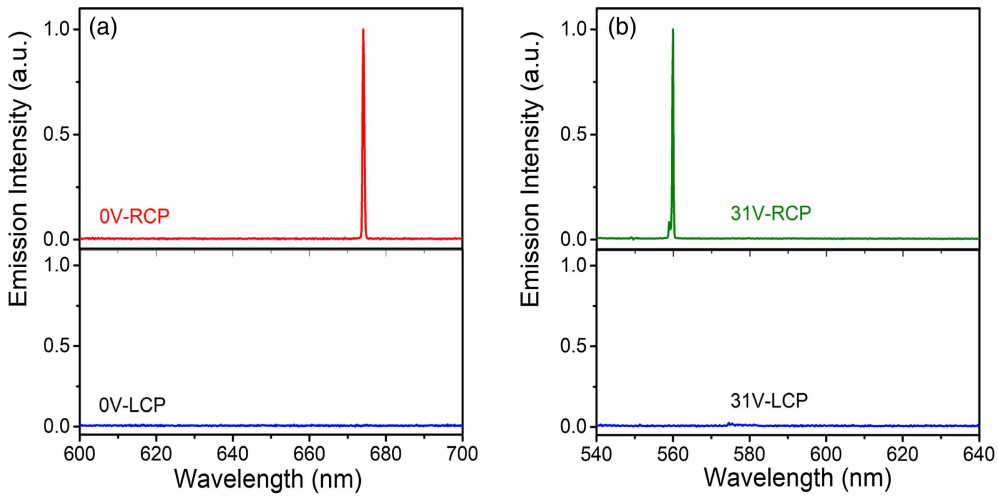

Fig. 7. Laser emission spectra of the dye-doped PSCLC measured for right-handed and left-handed circularly polarized (RCP and LCP, respectively) states under 0 V and 31 V, respectively.

The wavelength of the laser could be tuned reversibly in a wide spectral range, from 558 to 673 nm, by controlling the pitch gradient through DC electric fields. The principal advantage of the electrically controlled PSCLC laser is that the electric field is applied parallel to the helical axis and changes the pitch gradient instead of rotating this helix axis, thus preserving the heliconical structure during lasing. The preserved regular heliconical structure explains why the circular dissymmetry factor of lasing is high for the entire tunable range of emission. The optically pumped PSCLC laser is very simple to fabricate and operate, as it consists only of a thin slab of PSCLC material doped with a dye, confined between two glass plates with transparent electrodes. The PSCLC laser, with advantages including a wide tunable range, self-restoration, and rapid response and stability, coupled with its miniature size and narrow linewidths, may have diverse applications in intelligent optoelectronic devices.

Funding. National Natural Science Foundation of China (NSFC) (11404087, 11574070, 11874012, 51573036, 51703047, 61107014); Natural Science Foundation of Anhui Province (1708085MF150); Distinguished Youth Foundation of Anhui Province (1808085J03); Fundamental Research Funds for the Central Universities (JZ2017HGTB0187, JZ2018HGPB0276); European Union's Horizon 2020 research and innovation programme, H2020 Marie Skłodowska-Curie Actions (MSCA) (744817); Project of State Key Laboratory of Environment-Friendly Energy Materials, Southwest University of Science and Technology (SWUST) (17FKSY0109); Anhui Province Key Laboratory of Environment-Friendly Polymer Materials (KF2019001); China Postdoctoral Science Foundation (2015M571918, 2017T100442).

REFERENCES

1. A. D. Ford, S. M. Morris, and H. J. Coles, "Photonics and lasing in liquid crystals," Mater. Today **9**, 36–42 (2006).
2. H. Coles and S. Morris, "Liquid-crystal lasers," Nat. Photonics **4**, 676–685 (2010).
3. M. Mitov, "Cholesteric liquid crystals with a broad light reflection band," Adv. Mater. **24**, 6260–6276 (2012).
4. I. Muševič, "Liquid-crystal micro-photonics," Liq. Cryst. Rev. **4**, 1–34 (2016).
5. V. I. Kopp, B. Fan, H. K. M. Vithana, and A. Z. Genack, "Low-threshold lasing at the edge of a photonic stop band in cholesteric liquid crystals," Opt. Lett. **23**, 1707–1709 (1998).
6. Y. Zhou, Y. Huang, and S.-T. Wu, "Enhancing cholesteric liquid crystal laser performance using a cholesteric reflector," Opt. Express **14**, 3906–3916 (2006).
7. M. Uchimura, Y. Watanabe, F. Araoka, J. Watanabe, H. Takezoe, and G. Konishi, "Development of laser dyes to realize low threshold in dye-doped cholesteric liquid crystal lasers," Adv. Mater. **22**, 4473–4478 (2010).
8. P. V. Shibaev, V. I. Kopp, and A. Z. Genack, "Photonic materials based on mixtures of cholesteric liquid crystals with polymers," J. Phys. Chem. B **107**, 6961–6964 (2003).
9. A. Chanishvili, G. Chilaya, G. Petriashvili, R. Barberi, R. Bartolino, G. Cipparrone, A. Mazzulla, R. Gimenez, L. Oriol, and M. Pinol, "Widely tunable ultraviolet-visible liquid crystal laser," Appl. Phys. Lett. **86**, 051107 (2005).
10. K. Sonoyama, Y. Takanishi, K. Ishikawa, and H. Takezoe, "Position-sensitive cholesteric liquid crystal dye laser covering a full visible range," Jpn. J. Appl. Phys. **46**, L874–L876 (2007).
11. S. Furumi and N. Tamaoki, "Glass-forming cholesteric liquid crystal oligomers for new tunable solid-state laser," Adv. Mater. **22**, 886–891 (2010).
12. K. Funamoto, M. Ozaki, and K. Yoshino, "Discontinuous shift of lasing wavelength with temperature in cholesteric liquid crystal," Jpn. J. Appl. Phys. **42**, L1523–L1525 (2003).
13. J. Schmidtke, S. Kniesel, and H. Finkelmann, "Probing the photonic properties of a cholesteric elastomer under biaxial stress," Macromolecules **38**, 1357–1363 (2005).
14. A. Varanytsia, H. Nagai, K. Urayama, and P. Palffy-Muhoray, "Tunable lasing in cholesteric liquid crystal elastomers with accurate measurements of strain," Sci. Rep. **5**, 17739 (2015).
15. T.-H. Lin, Y.-J. Chen, C.-H. Wu, A. Y. G. Fuh, J. H. Liu, and P. C. Yang, "Cholesteric liquid crystal laser with wide tuning capability," Appl. Phys. Lett. **86**, 161120 (2005).
16. H. K. S. Finkelmann, A. Munoz, P. Palffy-Muhoray, and B. Taheri, "Tunable mirrorless lasing in cholesteric liquid crystalline elastomers," Adv. Mater. **13**, 1069–1072 (2001).
17. Z.-G. Zheng, B.-W. Liu, L. Zhou, W. Wang, W. Hu, and D. Shen, "Wide tunable lasing in photoresponsive chiral liquid crystal emulsion," J. Mater. Chem. C **3**, 2462–2470 (2015).

18. B.-W. Liu, Z.-G. Zheng, X.-C. Chen, and D. Shen, "Low-voltage-modulated laser based on dye-doped polymer stabilized cholesteric liquid crystal," Opt. Mater. Express **3**, 519–526 (2013).
19. M. Ozaki, M. Kasano, T. Kitasho, D. Ganzke, W. Haase, and K. Yoshino, "Electro-tunable liquid-crystal laser," Adv. Mater. **15**, 974–977 (2003).
20. H. Yu, B. Y. Tang, J. Li, and L. Li, "Electrically tunable lasers made from electro-optically active photonics band gap materials," Opt. Express **13**, 7243–7249 (2005).
21. B. Park, M. Kim, S. W. Kim, W. Jang, H. Takezoe, Y. Kim, E. H. Choi, Y. H. Seo, G. S. Cho, and S. O. Kang, "Electrically controllable omni-directional laser emission from a helical-polymer network composite film," Adv. Mater. **21**, 771–775 (2009).
22. Y. Inoue, H. Yoshida, K. Inoue, Y. Shiozaki, H. Kubo, A. Fujii, and M. Ozaki, "Tunable lasing from a cholesteric liquid crystal film embedded with a liquid crystal nanopore network," Adv. Mater. **23**, 5498–5501 (2011).
23. M. Wang, C. Zou, J. Sun, L. Zhang, L. Wang, J. Xiao, F. Li, P. Song, and H. Yang, "Asymmetric tunable photonic bandgaps in self-organized 3D nanostructure of polymer-stabilized blue phase I modulated by voltage polarity," Adv. Funct. Mater. **27**, 1702261 (2017).
24. S. Furumi, S. Yokoyama, A. Otomo, and S. Mashiko, "Electrical control of the structure and lasing in chiral photonic band-gap liquid crystals," Appl. Phys. Lett. **82**, 16–18 (2003).
25. G. Strangi, V. Barna, R. Caputo, A. De Luca, C. Versace, N. Scaramuzza, C. Umeton, R. Bartolino, and G. N. Price, "Color-tunable organic microcavity laser array using distributed feedback," Phys. Rev. Lett. **94**, 063903 (2005).
26. S. P. Palto, L. M. Blinov, M. I. Barnik, V. V. Lazarev, B. A. Umanskii, and N. M. Shtykov, "Photonics of liquid-crystal structures: a review," Crystallogr. Rep. **56**, 622–649 (2011).
27. J. Xiang, A. Varanytsia, F. Minkowski, D. A. Paterson, J. M. D. Storey, C. T. Imrie, O. D. Lavrentovich, and P. Palffy-Muhoray, "Electrically tunable laser based on oblique heliconical cholesteric liquid crystal," Proc. Natl. Acad. Sci. USA **113**, 12925–12928 (2016).
28. G. H. Heilmeier and L. A. Zanoni, "Guest-host interactions in nematic liquid crystals. A new electro-optic effect," Appl. Phys. Lett. **13**, 91–92 (1968).
29. V. G. Rumyantsev, A. V. Ivashchenko, V. M. Muratov, V. T. Lazareva, E. K. Prudnikova, and L. M. Blinov, "Dyes with negative dichroism for liquid crystal displays based on the guest-host effect," Mol. Cryst. Liq. Cryst. **94**, 205–212 (2007).
30. Q. Liu, Y. Yuan, and I. I. Smalyukh, "Electrically and optically tunable plasmonic guest-host liquid crystals with long-range ordered nanoparticles," Nano Lett. **14**, 4071–4077 (2014).
31. K. M. Lee, V. P. Tondiglia, M. E. McConney, L. V. Natarajan, T. J. Bunning, and T. J. White, "Color-tunable mirrors based on electrically regulated bandwidth broadening in polymer-stabilized cholesteric liquid crystals," ACS Photon. **1**, 1033–1041 (2014).
32. H. Nemati, S. Liu, R. S. Zola, V. P. Tondiglia, K. M. Lee, T. White, T. Bunning, and D.-K. Yang, "Mechanism of electrically induced photonic band gap broadening in polymer stabilized cholesteric liquid crystals with negative dielectric anisotropies," Soft Matter **11**, 1208–1213 (2015).
33. K. M. Lee, V. P. Tondiglia, and T. J. White, "Photosensitivity of reflection notch tuning and broadening in polymer stabilized cholesteric liquid crystals," Soft Matter **12**, 1256–1261 (2016).
34. S. M. Wood, J. A. J. Fells, S. J. Elston, and S. M. Morris, "Wavelength tuning of the photonic band gap of an achiral nematic liquid crystal filled into a chiral polymer scaffold," Macromolecules **49**, 8643–8652 (2016).
35. K. M. Lee, V. P. Tondiglia, N. P. Godman, C. M. Middleton, and T. J. White, "Blue-shifting tuning of the selective reflection of polymer stabilized cholesteric liquid crystals," Soft Matter **13**, 5842–5848 (2017).
36. M. Yu, L. Wang, H. Nemati, H. Yang, T. Bunning, and D.-K. Yang, "Effects of polymer network on electrically induced reflection band broadening of cholesteric liquid crystals," J. Polym. Sci. B **55**, 835–846 (2017).